The Emergent Connectome in *Caenorhabditis elegans* Embryogenesis

DevoWorm Group[1], Bradly Alicea[2,3]

KEYWORDS: Connectomics, Networks, Embryogenesis, Systems Biology, Data Science

ABSTRACT

The relatively new field of connectomics provides us with a unique window into nervous system function. In the model organism *Caenorhabditis elegans*, this promise is even greater due to the relatively small cellular size (302 cells) of the nervous system. While the adult *C. elegans* connectome has been characterized, the emergence of these networks in development has yet to be established. In this paper, we approach this problem using secondary data describing the birth times of terminally-differentiated cells as they appear in the embryo and connectomics data for pharyngeal nervous system cells in the adult hermaphrodite. By combining these two sources of data, we can better understand patterns that emerge in an incipient connectome. This includes identifying at what point in embryogenesis the cells of a connectome first comes into being, observing some of the earliest neuron-neuron interactions, and making comparisons between the formally-defined connectome and the embryogenetic interactome. An analysis is also conducted to root terminally-differentiated pharyngeal cells in their developmental cell lineage. This analysis reveals subnetworks with different properties at 300 minutes of embryogenesis. Overall, this analysis reveals important information about the birth order of specific cells, key building blocks of global connectivity, and how these structures corresponds to various embryogenetic stages during the emergence of a connectome.

INTRODUCTION

Connectomics can tell us a lot about the way behavior is generated from networks of neurons such as the central nervous system or retina (Seung, 2012; Helmstaedter et.al, 2013). This pattern of connectivity is hard to understand in mammalian brains (Morgan and Lichtman, 2014), but in the nematode *C. elegans*, the connectomics of a 302 cell nervous system can be easily visualized and analyzed. With its relatively small size and single-cell specificity, the *C. elegans* connectome serves as a model for function relative to more complex nervous systems (Chatterjee and Sinha, 2007). As such, data describing *C. elegans* connectivity are easily available in an accessible computational format and storage repository (see Methods). The *C. elegans* connectome has been formally-defined as a connectivity matrix by Jarrell et.al (2012) and Varshney et.al (2011). Previous attempts at characterizing the connectome in *C. elegans* has focused on the static adult version. Yet we can also combine connectome data with cellular data from embryogenesis to yield a dynamic version of the connectome as it emerges from developmental cells.

Embryogenetic connectomics allows us to look at the connectome as it emerges in development. This includes partitioning the connectome by embryonic time interval and developmental cell sublineage of origin to potentially discover the origin of modules and functional subdivisions in the adult connectome (Kaiser, 2011; Reigl et.al, 2004). By using *C. elegans* as a model organism, we can also make connections between the interactome of developmental cell lineages and adult neuronal network topologies. One benefit of combining multiple datasets is to investigate previously unexplored areas of inquiry not possible by relying

[1] For past and current list of contributors, please see the group website: http://devoworm.weebly.com
[2] Orthogonal Research, Champaign, IL bradly.alicea@outlook.com
[3] OpenWorm Foundation, Boston, MA

on a single dataset or model (Faisal et.al, 2014). Making an explicit link between the connectome and interactome provides clues as to which relationships between developmental cells (such as spatial clusters and embryogenetic asymmetry) also give rise to neuronal cell-neuronal cell connectivity (Varier and Kaiser, 2011).

In this paper, we will investigate the interactome of a selected time interval in the embryo using a complex network approach. Then, we will combine previously published connectome (Varshney et.al, 2011) data with a bioinformatic approach (DevoWorm, 2017) to establish the connections between the process of developmental cell differentiation and terminally-differentiated cells emerging into a coherent nervous system. This will yield a series of time-dependent networks in addition to insights regarding how the embryogenetic process influences the formation of functional neuronal networks.

METHODS

Interactome data. Datasets consist of pre-hatching (up to 558 cells) cell divisions (Bao et.al, 2008). During acquisition of these data, cell nucleus identification was done by identifying GFP+ markers using the Starry Night software package. Three- dimensional (spatial) position and nomenclature (identity) for all cells are extracted in this manner from 261 embryos. The position of each cell is averaged across all embryos along each anatomical axis (anterior-posterior, left-right, and dorsal-ventral). The positional data is then translated to have its origin at the location of the P0 cell, which produces a three-dimensional spatial representation of the embryo.

Embryonic Time Series. To construct the embryonic time series, timed cell lineage data were acquired courtesy of Nikhil Bhatla and his Interactive lineage tree application (http://wormweb.org/celllineage). Cells represented in an embryo at a given time are determined by first calculating the lifespan of each cell in the lineage tree (e.g. the time at which each cell is born and each cell either divides or dies), and then identifying all cells alive at a given time. Terminally-differentiated cells were assumed never to die, unless specified by the data. These data were also used to establish a link between developmental cell sublineages and terminally-differentiated cells.

Connectome data. The connectome data was provided by the Open Connectome database (http://openconnecto.me/). The connectome data originated with pharyngeal nervous system cells (n = 279) from the adult hermaphrodite (Varshney et.al, 2011). The connectivity matrix with electrical synaptic weights were matched against our list of terminally-differentiated cells at 280, 290, 300, and 400 minutes. The resulting cells were used to create unique connectivity matrices for each timepoint, and included unconnected cells. These data were visualized in Gephi 0.9.0 and modeled using yED. Adjacency matrices were also created from the connectivity information. All files (r code, GraphML code, and data files) are available at https://github.com/devoworm/embryogenetic-connectome.

The adjacency matrix data provided in Varshney et.al (2011) was extracted from previously collected electron micrographs (White et.al, 1986). The network adjacency matrices in this paper are defined and weighted by electrical synapses called gap junctions (Majewska and Yuste, 2001),

but is ordered by the additional existence of chemical synapses. The gap junction-based weights are determined by the number of gap junctions shared between a pair of cells.

Pharyngeal connectome modeling in adult phenotype. The lateral-view digital model of the hermaphrodite adult *C. elegans* using the Supplemental Figure 1 and Supplemental Figure 2 originates from the Virtual Worm project. The original model was constructed using Blender (available at http://canopus.caltech.edu/virtualworm/Virtual%20Worm%20Blend%20File/), and the annotated Blender model (with pharyngeal connectome data included as a series of scenes) is available at https://github.com/devoworm/embryogenetic-connectome/blob/master/developmental-connectome-265-300-minutes-adult-model.blend

Distance Metric

To calculate a relational distance between three-dimensional cell positions, a generalized Euclidean distance metric (D) was used. This distance was then normalized in the form of an index (d_i), which takes all distances as a proportion of the maximum distance between cells in the embryo. These metrics are defined mathematically as

$$\mathrm{D} = \sqrt{\mathrm{x}^2} + \mathrm{y}^2 + \mathrm{z}^2 \qquad \textbf{[1]}$$

$$d_i = \left(\frac{D_i}{\max(D_i)}\right) \qquad \textbf{[2]}$$

A symmetric matrix of indexed relational distances is then used to construct an unordered network of all nodes in the lineage tree. This matrix can then be partitioned by subtree or level. A threshold T is used to restrict the analysis to all values below a certain index value (e.g. 0.05).

All cells in the interactome networks are derived from the averaged *x,y,z* positions of cell centroids and the distances between these centroids along each dimension. The greater the distance between centroids of neighboring cells, the larger the cells in that region. Increasingly larger distances between cell centroids represents correspondingly larger distances across the embryo. A value of 1.0 for the index d_i represents the maximal extent of the embryo, and represents the distance between cells at opposite ends of the embryo. The index d_i is also asymptotic to 0.0 as a distance metric, as all self-connections have a value of 0.0. These values are removed from the analysis for all thresholds T.

RESULTS

Interactome in Embryo

To provide a comparator for the pharyngeal connectome networks, an interactome was constructed for all cells in the 128 terminal-cell lineage tree (a total of 110 cells). This network represents all cells resulting from seven division events after fertilization. At this point in developmental time (130-165 minutes), the relationships between cells should exhibit left-right modularity based on a cell's ancestor in the 2-cell embryo, and should also exhibit adjacency depending on their closeness to the embryo midline.

A network was constructed using two distance thresholds: T = 0.05 and T = 0.02. Smaller thresholds result from smaller neighboring cells. We test this for two distance thresholds: T = 0.05 and T = 0.02. The visualization of these networks as circular plots is shown in Figure 1. Nodes (representing each developmental cell) are separated by a cell's bipartite sublineage (e.g. AB and P1). It is apparent that while connectivity is well-distributed within and between sublineages at T = 0.05, this is not the case for T = 0.02. Table 1 summarizes these differences in a quantitative fashion.

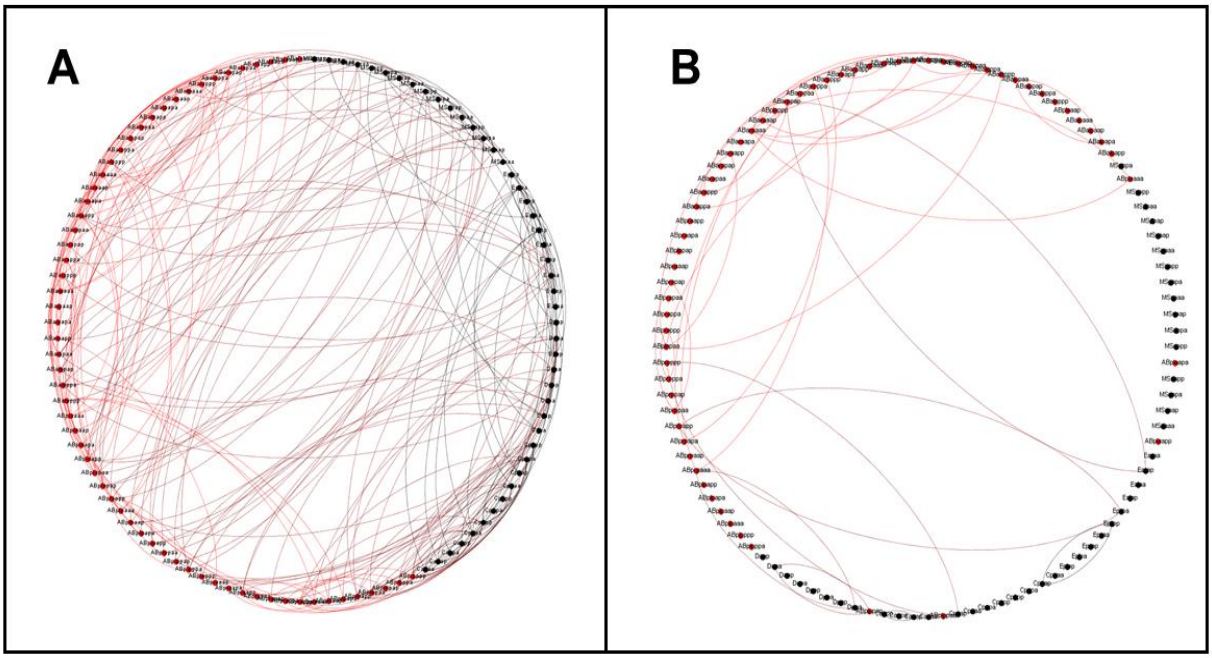

Figure 1. Circular graph of the embryonic interactome for the 128 terminal-cell lineage tree (N=224). A) Euclidean distance threshold at T = 0.05. AB sublineage nodes are in red, P1 sublineage nodes are in blue. B) Euclidean distance threshold at T = 0.02. AB sublineage nodes are in red, P1 sublineage nodes are in blue.

In Table 1, it is apparent that very small distances (T → 0) reveal differences in connectivity between sublineages. In general, cells descending from P1 are larger and less likely to be adjacent to cells descending from AB. Our analysis also demonstrates that cell size is asymmetric between sublineages and even between small groups of developmental cells that will eventually become neurons. Both Table 2 and Figure 2 focuses on the asymmetries of connectivity in the AB sublineage.

Table 1. Matrix of inter- and intra-subtree connectivity at T = 0.05 (n = 290) and T = 0.02 (n = 44) for 128-terminal cell lineage tree (N=224).

	AB		**P1**	
	T = 0.05	**T = 0.02**	**T = 0.05**	**T = 0.02**
AB	104 (36%)	30 (68%)	112 (38%)	10 (23%)
P1	112 (38%)	10 (23%)	74 (26%)	4 (9%)

Within the AB sublineage are four sublineages representing the octopartite lineage tree (descendents of the 8 terminal-cell lineage tree): ABpl, ABpr, ABal, and ABar. We show inter- and intra- subtree connectivity patterns in tabular (Table 2) and graphical (Figure 2) form. This analysis of the 128 terminal-cell lineage tree was analyzed at T = 0.02. There are notable asymmetries amongst these cells. For example, a large majority of the inter-sublineage connections involve the ABar sublinage. Also, sublineage ABpl exhibits no intra-sublineage connections. These relationships become important as all terminally-differentiated neurons in the pharyngeal connectome originate from developmental cells in the AB sublineage.

Table 2. Matrix of inter- and intra-subtree connectivity within the AB subtree at T = 0.02 (n = 44) for 128 terminal-cell lineage tree (N=224).

	ABpl	**ABpr**	**ABal**	**ABar**
ABpl	0%	0%	3%	6.7%
ABpr	0%	13%	0%	6.7%
ABal	3%	0%	20%	0.1
ABar	6.7%	6.7%	10%	13%

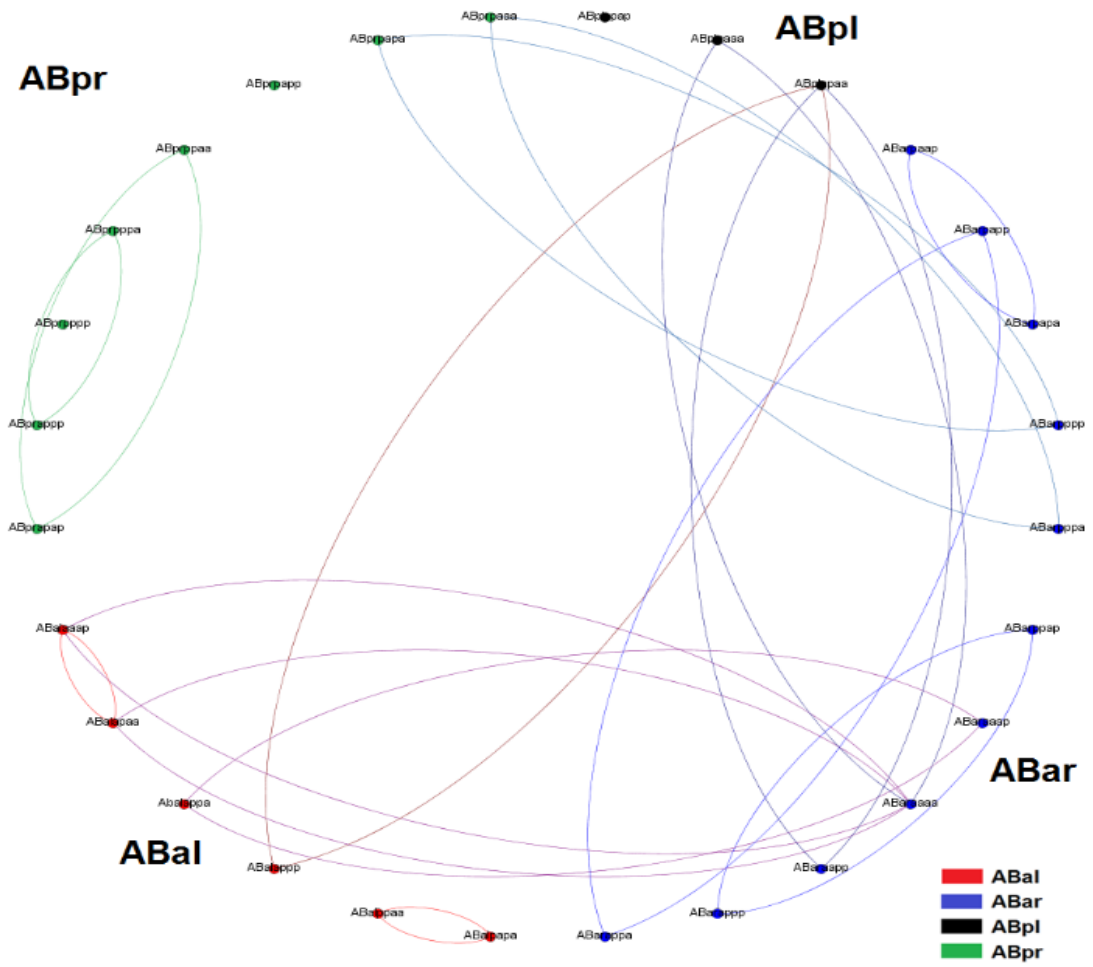

Figure 2. Circular graph of the embryonic interactome for the 128-cell lineage tree (N=224), Euclidean distance threshold at T = 0.02. Nodes are color-coded by the four AB sublineages in an 8-cell lineage tree.

Neural Connectome in Embryo

Once developmental cells from the AB lineage terminally differentiate, some of them become neurons in the pharynx. These pharyngeal cells exhibit synaptic interconnections, and the extent of their connectivity may be determined by their proximity. By combining connectomic data from Varshney (2011) and terminally differentiated cell birth times from DevoWorm (2017), we construct pharyngeal connectome for three time points of interest: 280, 290, and 300 minutes of embryogenesis. These time points were selected for their emphasis on the emergence of pharyngeal cells and their connectivity during this time period. As has just been demonstrated, only developmental cells are generated before 200 minutes. Yet by 400 minutes, all terminally differentiated cells not generated post-embryonically are also present in the developmental time-series.

Figure 3 demonstrates the first stage of connectivity in the pharyngeal connectome. The earliest coherent pharyngeal connectome (cells with synaptic connectivity) emerges at 280 minutes of embryogenesis. The first neuronal cell to emerge in pharyngeal connectome (RMEV at 265 minutes) is also disconnected from a network of five other neurons at 280 minutes. These four connected neurons reveal another interesting attribute of early connectomes. Neuronal cells often emerge in pairs (e.g. symmetrical components), and become reciprocally interconnected. In the vast majority of cases, these involve left-right pairs. Bilateral reciprocity becomes a motif in these early networks, and a means to build more complex connectivity patterns later on.

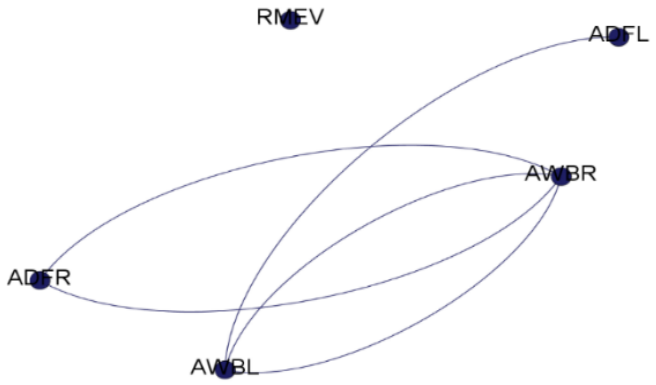

Figure 3. The pharyngeal connectome at 280 minutes. Blue nodes are all terminally-differentiated cells born by 280 minutes of embryogenesis.

Figure 4 and 5 show the pharyngeal connectome at 290 and 300 minutes, respectively. Aside from denser and more complex connectivity patterns, the weights of synaptic connection increase while also exhibiting greater variation during and after 300 minutes. One-way and reciprocal binary connectivity now combine to form motifs while also serving as a means to build more complex connectivity patterns later on. For example, while RMEV was unconnected at 280 minutes, RMEV becomes connected to several neurons emerging at 290 minutes. This increase in connectivity is enough for RMEV to become a regional hub in the network.

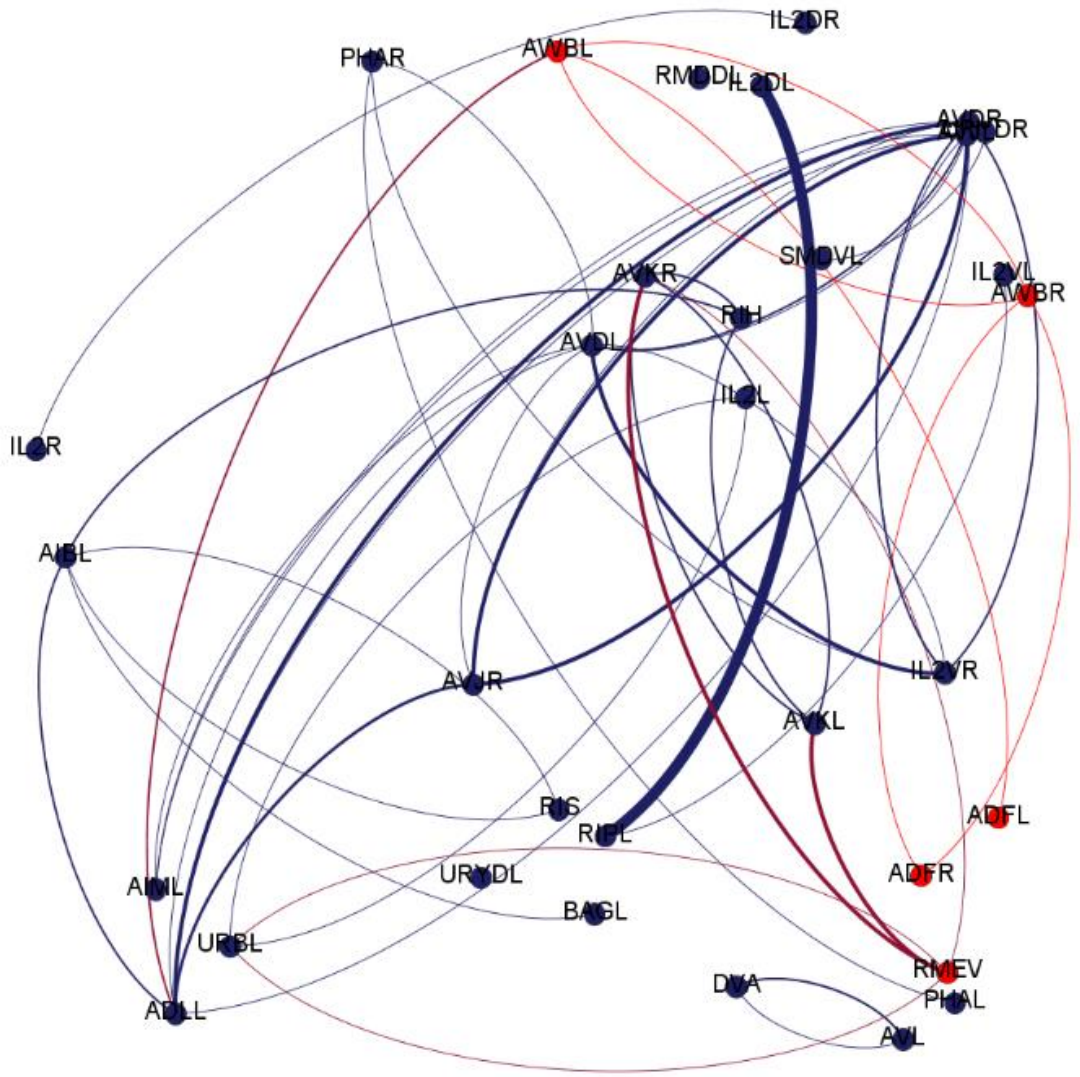

Figure 4. The pharyngeal connectome at 290 minutes. Red nodes are all terminally-differentiated cells born by 280 minutes of embryogenesis, and blue nodes are all terminally-differentiated cells born by 290 minutes of embryogenesis.

To better understand how motifs and patterns of connectivity are formed in the pharyngeal connectome over time, several proportions are calculated for four timepoints (280, 290, 300, and 400 minutes). The results are shown in Table 3, and looking at the trends for reciprocal connections per timepoint and proportion of source and target nodes per timepoint yields an interesting relationship. At 280 minutes, we observe a few reciprocally-connected neurons that make up the entirety of the network. By 290 minutes, about 30 additional neurons are born, many of which only have an input or output, and many of those lacking a bilateral counterpart. At 300 minutes, many

these cells gain input and/or output connections that make them more fully functioning members of the network. Once we reach 400 minutes, many more cells are born that serve as bilateral counterparts to existing cells. Thus, the 280-300 minute period is defined by asymmetric connectivity patterns, while from 300 minutes on network connectivity becomes more complex, as feedback loops and cliques are assembled. A visualization of the cells born at each time point on a 3-dimensional model of the adult hermaphrodite is shown in Supplemental File 1, and an animation showing expansion of the connectome in the context of both the adult hermaphrodite and network visualizations is shown in Supplemental File 2.

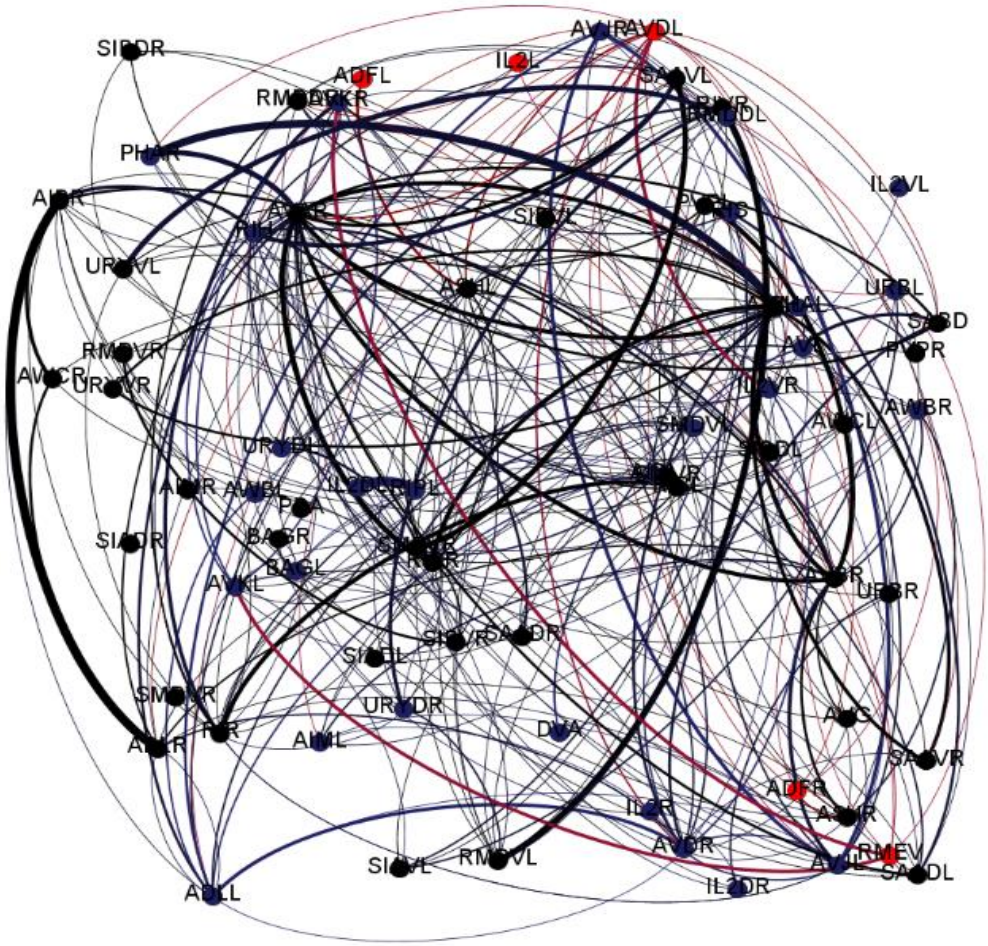

Figure 5. The pharyngeal connectome at 300 minutes. Red nodes are all terminally-differentiated cells born by 280 minutes of embryogenesis, black nodes are all terminally-differentiated cells born by 290 minutes of embryogenesis, and blue nodes are all terminally-differentiated cells born by 300 minutes of embryogenesis.

Origin of terminally-differentiated pharyngeal cells

The pharyngeal connectome can be analyzed in two ways: a dynamic version, and a static version that explicitly demonstrates linkages with developmental cell lineages. To render the latter,

we took all cells in the pharyngeal connectome dataset and matched them in two ways. The first match involved taking all cells in the pharyngeal connectome dataset and matching them to cells from the 300 minute point in our embryogenetic time series. The second match involved taking each cell resulting from this intersection operation and linking to its corresponding 8-cell embryo ancestor representing the developmental cell lineage. This resulted in a classification of the pharyngeal cell matches. Figures 6 and 7 show the resulting graphs. Figure 6 shows the entire pharyngeal connectome for four subtrees at 300 minutes of embryogenesis. On the left is the full connectivity of this connectome, while on the right all connections above a nominal threshold are shown. In the thresholded case, some cells retain their connectivity and serve as network hubs, while other node become disconnected.

Table 3. Number of reciprocal connections (ordered connections from cell A to cell B and from cell B to cell A) and nodes connected to network serving as both sources and targets.

	280	**290**	**300**	**400**
Number of nodes	4	31	69	163
Reciprocal Connections	0.8	0.46	0.39	0.74
Source and Target Nodes	0.75	0.61	0.9	0.98

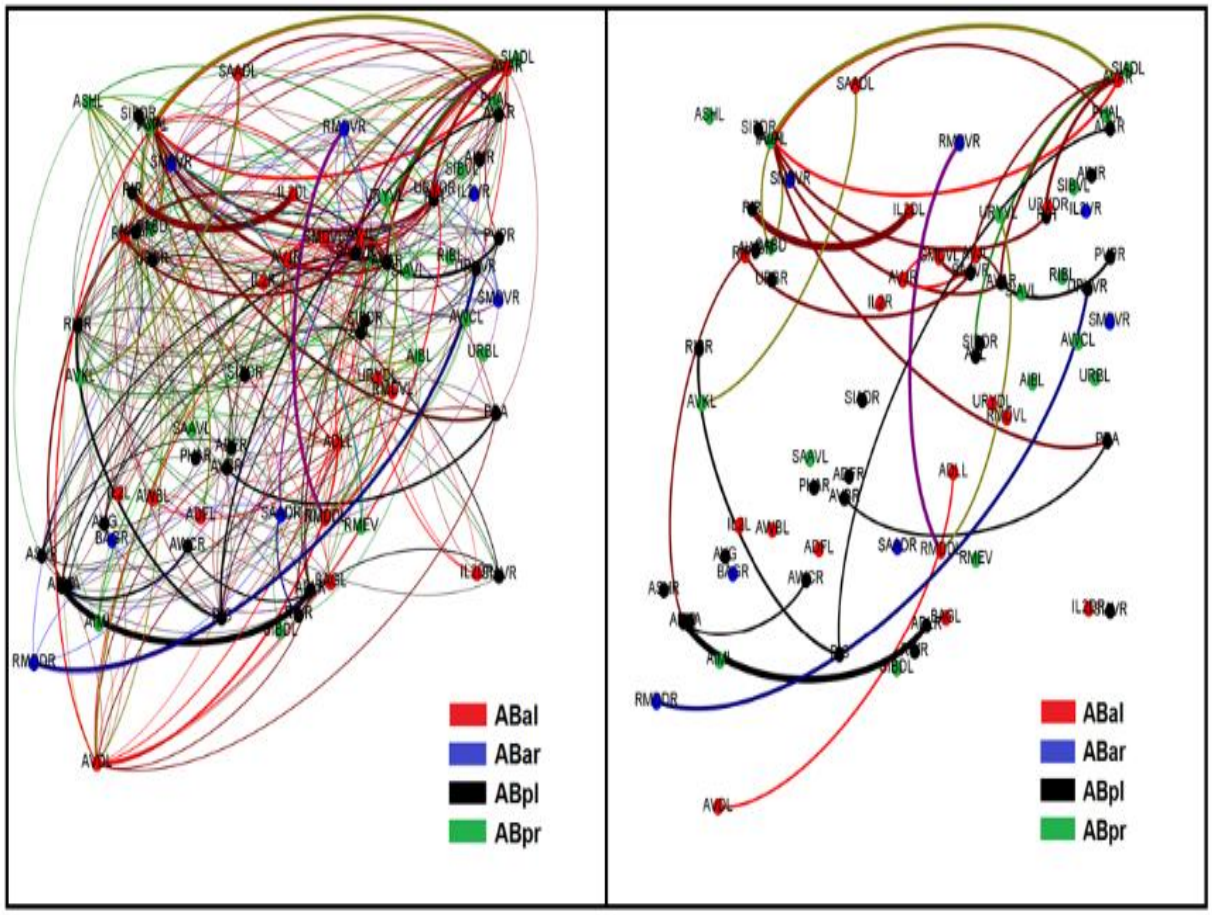

Figure 6. Pharyngeal connectome at 300 minutes of embryogenesis. LEFT: entire connectome, nodes are color coded by developmental cell sublineage of origin. RIGHT: edges with a value greater than 4.0, nodes are color coded by developmental cell sublineage of origin.

Table 4. Characterization of connections amongst neurons by developmental subtree of origin emerging between 300 and 400 minutes of embryogenesis. Network generated using a synaptic threshold of 4.0.

	Source	Source only	Target	Target only	Both
ABal	32	22	39	29	10
ABpl	26	18	25	17	8
ABar	10	10	2	2	0
ABpr	27	16	36	25	11
Caap	6	6	0	0	0

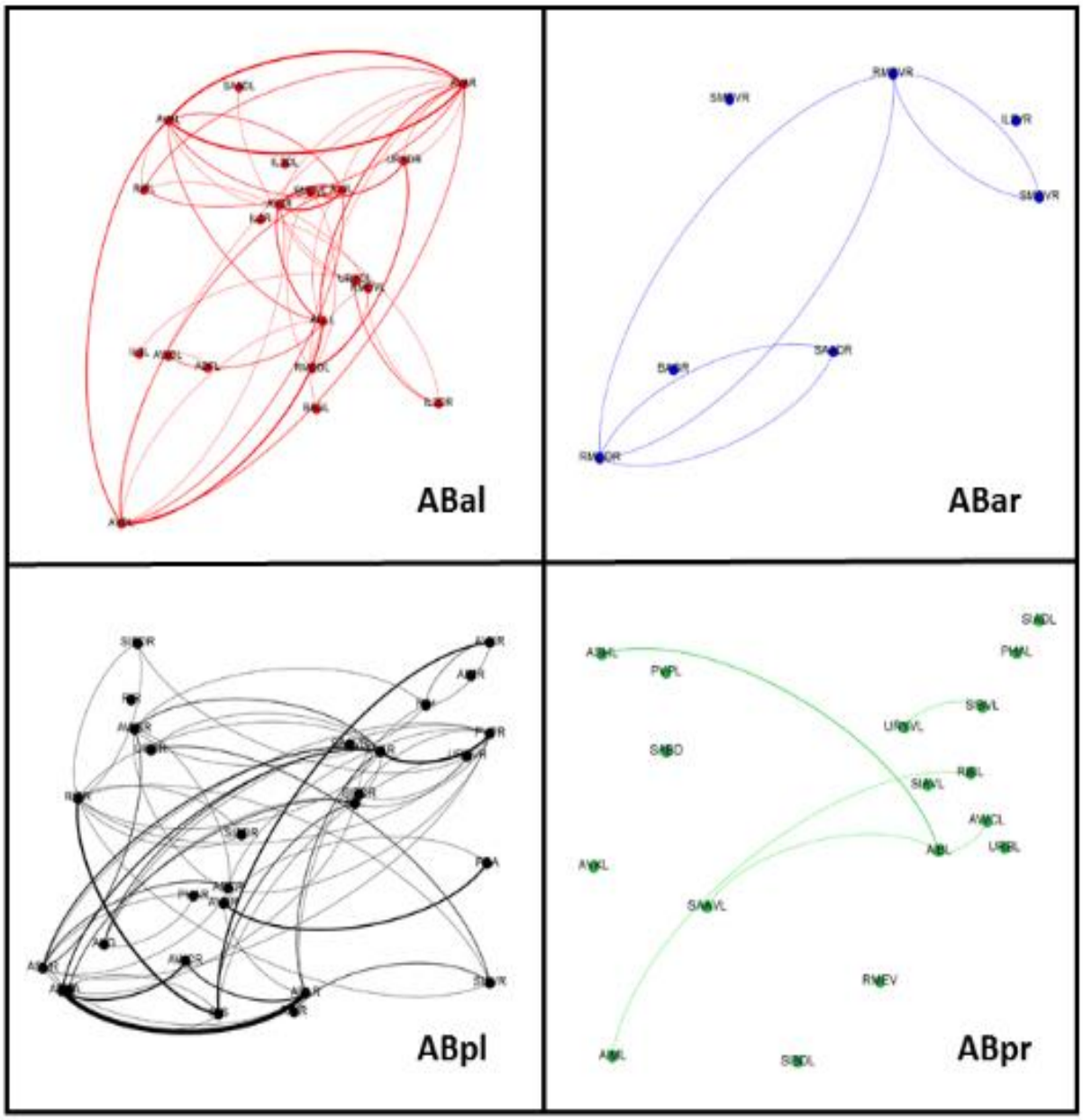

Figure 7. Connectivity at 300 minutes of embryogenesis by developmental cell of origin. Terminally-differentiated cells that descend from four cells in the 8-cell embryo.

A visualization of the information in Figures 6 and 7 (cells derived from different developmental sublineages at 300 minutes of embryogenesis) on a 3-dimensional model of an adult hermaphrodite is shown in Supplemental File 1. Given the concurrence of neuronal and developmental information, there are a few observations we can make. First, most pharyngeal cells at 300 minutes of embryogenesis derive from either the ABal or ABpl lineage. Secondly, neurons that derive from the ABal developmental sublineage begin to form a clique with a core of connected cells. To understand the role of developmental cell lineage of origin in connectivity at 300 minutes, we can look at descendants of each developmental cell sublineage to look at patterns of connectivity (Figure 7). Without thresholding the connections between cells, we can see that disconnected cells exist among descendants of sublineages ABar and ABpr only. The interconnections amongst these subnetworks are less dense than subnetworks representing ABal and ABpl. When the pharyngeal connectome is thresholded, cells from all sublineages (ABal, ABar, ABpl, and ABpr) become disconnected (Figure 6, Right). However, a terminally differentiated cell's time of birth has no bearing on connectivity patterns.

Finally, we would like to visualize the data to gain more information about the locations of these cells in context of the adult phenotype. We can model the pharyngeal connectome using a lateral-view model of the adult hermaphrodite over both developmental time (Supplemental File 2) and across developmental sublineages of origin (Supplemental File 3). While the lateral view shows the relative positions of cells along an orientation representing the lineage tree, this model also obscures spatial structure along the left-right axis. To do this, we used the data used to produce SF2 and counted all cells that are part of a bilateral pair and their laterality in their terminally differentiated position. For the ABar subtree, all cells (7 of 7) are on the right-hand side. The ABpl subtree yields 20 of 28 cells on the right-hand side and 1 of 18 cells on the left-hand side. The remaining AB sublineages are biased towards the left-hand side: in ABpr, 15 of 17 cells are on the left-hand side, while ABal contains 15 of 20 cells on the left-hand side and only 5 of 20 cells on the right-hand side.

DISCUSSION

We have been able to demonstrate the developmental origins of the pharyngeal connectome, a network that emerges from the first terminally-differentiation neurons in *C. elegans* and is shaped by their ancestral developmental cell lineages and the proximal relationships between these cells. These relationships form their own network (interactome) which provides an earlier developmental reference point for the growing connectome. Finally, there is the linkage between network topologies representing developmental and terminally-differentiated cells. This brings us back to developmental cell lineages and a comparison to adult pharyngeal cells. Since connectivity in the neural connectome is determined by the existence of gap junctions between cells, there should be a spatial similarity in connectivity patterns between the embryonic interactome and the pharyngeal connectome.

Our connectome data are bounded by the 200 to 400 minute interval, which is the time between the first appearance of non-germline terminally differentiated cells and the comma stage of development (Chisholm and Hardin, 2005). The pharyngeal connectome first emerges at 280 minutes, and grows quickly before up to the 40 minute mark. Within this span of time, the pharyngeal connectome transitions from a simple interconnected set of neurons to a complex network. In the original analysis of the connectome data (Varshney et.al, 2011), up to 11 types of

motifs were identified in the full pharyngeal network based on gap junctions. While we did not conduct a motif analysis on these data, we can still observe rudimentary motifs and related patterns, particularly the emergence of reciprocally connected pairs, disconnected cells, and even preferential attachment (Betzel et.al, 2016).

Comparisons between the developmental interactome, pharyngeal connectome, and developmental cell identity yield broad trends. One of these trends is an asymmetry in the pharyngeal connectome by developmental cell sublineage. When we partition cells in the connectome by developmental cell origin, these groups of cells exhibit differential connectivity densities both within and between the partitioned subnetworks. Making a comparison between Table 2 (embryonic interactome) and Table 4 (pharyngeal connectome) shows results that vary by developmental cell subtree. On the one hand, developmental subtrees ABal and ABpr exhibit somewhat consistent patterns of intra- and inter-subtree connectivity between the interactome and connectome. On the other hand, the comparative results for ABpl and ABar demonstrate either an opposite pattern of connectivity (ABpl) or a consistent sparsity (ABar). In particular, ABal is notable for its high degree of connectivity for the pharyngeal connectome and sparse connectivity for the embryonic interactome.

One way to interpret these results is to consider what is happening at 280 to 400 minutes of embryogenesis, and in particular the interval from 280 to 300. We have observed that the first proto-connectome emerges at 280 minutes of embryogenesis. We have also observed that the emergence of hub neurons occurs between 290 and 300 minutes of embryogenesis. During this brief period of time, the embryo undergoes its first cleavage at 280 minutes (Soto et.al, 2002) with dorsal intercalation and ventral cleft closure occurring by 290 minutes (Sulston et.al, 1983; Altun and Hall, 2011). The conventional wisdom is that all pharyngeal cells are generated during the first proliferation phase (Altun and Hall, 2011). We can refine this finding by suggesting that the connectome first proliferates between 280 and 300 minutes, and continues to grow in size until the 400 minute mark. At this point, the pharyngeal connectome appears to be structurally complete. This is consistent with the finding that the pharynx forms according to the rules of multi-step morphogenesis that exhibit collective cellular behaviors such as reorientation and contraction (Portereiko and Mango, 2001). For example, at the 310 minute mark, cell migrations such as the movement of dorsal hypodermal nuclei to the side of the midline opposite from their origin are taking place (Chisholm and Hardin, 2005). The 400 minute mark is also the beginning of the elongation phase and the end of the comma phase (Chisholm and Hardin, 2005).

There are a few caveats to consider, particularly in terms of pursuing future directions. One issue is that neuronal birth time is not particularly informative of the details of later synaptic connectivity (Kratsios et.al, 2015). It has previously been found that early-born neurons tend to be both more highly connected and exhibit more longer-range connections than later-born neurons (Varier and Kaiser, 2011). Yet neuronal birth time along with their developmental cell ancestry may be informative of later aggregate patterns in the *C. elegans* nervous system. As most neurons are present before hatching, contacts between adjacent neurons in early development might be important in establishing long-distance connectivity patterns (Varier and Kaiser, 2011). Future work might take into account the role of axonal projections and cell migrations in the process of assembling the adult connectome.

ACKNOWLEDGEMENTS

We would like to acknowledge all primary data donors (datasets specified in the Methods section), without which this paper would not be possible. Thanks also go to the OpenWorm Foundation, which provided institutional and intellectual support. Additional thanks go to past and current members of the DevoWorm group, information about which can be found at http://devoworm.weebly.com.

SUPPLEMENTAL MATERIALS

Supplemental Figure 1. Images of pharyngeal connectome cells (shown in blue) born by 300 minutes embryogenesis in the adult hermaphrodite *C. elegans* phenotype. From top: ABal, ABar, ABpl, and ABar sublineages.

Supplemental Figure 2. Images of pharyngeal connectome (shown in orange) cells born at the given time in embryogenesis in the adult hermaphrodite *C. elegans* phenotype. From top: 265, 280, 290, and 300 minutes.

Supplemental File 3. Animation showing expansion of the pharyngeal connectome in the context of both the adult hermaphrodite *C. elegans* phenotype and the unordered connectivity amongst cells in the expanding connectome.

REFERENCES

Altun, Z.F. and Hall, D.H. (2011). Nervous system, general description. In WormAtlas. doi:10.3908/wormatlas.1.18.

Bao, Z.R., Murray, J.I., Boyle, T., Ooi, S.L., Sandel, M.J., and Waterston, R.H. (2006). Automated cell lineage tracing in *Caenorhabditis elegans*. PNAS, 103, 2707-2712.

Betzel, R.F., Avena-Koenigsberger, A., Goni, J., He, Y., de Reus, M.A., Griffa, A., Vertes, P.E., Misic, B., Thiran, J-P., Hagmann, P., van den Heuvel, M., Zuo, X-N., Bullmore, E.T., and Sporns, O. (2016). Generative models of the human connectome. Neuroimage, 124(A), 1054–1064.

Chatterjee, N. and Sinha, S. (2007). Understanding the mind of a worm: hierarchical network structure underlying nervous system function in C. elegans. Progress in Brain Research, 168, 145–153.

Chisholm, A.D. and Hardin, J. (2005). Epidermal morphogenesis (December 01, 2005), WormBook, ed. The *C. elegans* Research Community, WormBook, doi/10.1895/wormbook.1.35.1, http://www.wormbook.org.

DevoWorm (2017). The Emergent Worm: dynamic cellular differentiation in the *Caenorhabditis elegans* embryogenesis.

Faisal, A., Peltonen, J., Georgii, E., Rung, J., and Kaski, S. (2014). Toward Computational Cumulative Biology by Combining Models of Biological Datasets. PLoS One, 9(11), e113053.

Jarrell. T.A., Wang, Y., Bloniarz, A.E., Brittin, C.A., Xu, M., Thomson, J.N., Albertson, D.G., Hall, D.H., and Emmons, S.W. (2012). The connectome of a decision-making neural network. Science, 337, 437-444.

Helmstaedter, M., Briggman, K.L., Turaga, S.C., Jain, V., Seung, H.S., and Denk, W. (2013). Connectomic reconstruction of the inner plexiform layer in the mouse retina. Nature, 500(7461), 168-174.

Hobert, O. (2014). Development of Left/Right Asymmetry in the *Caenorhabditis elegans* Nervous System: from zygote to postmitotic neuron. Genesis, 52, 528-543.

Hobert, O. (2005). Specification of the nervous system. WormBook, The *C. elegans* Research Community, ed. WormBook, doi/10.1895/wormbook.1.12.1.

Kaiser, M. (2011). A tutorial in connectome analysis: Topological and spatial features of brain networks. NeuroImage, 57(3), 892–907.

Kratsios, P., Pinan-Lucarre, B., Kerk, S-Y., Weinreb, A., Bessereau, J-L., and Hobert, O. (2015). Transcriptional coordination of synaptogenesis and neurotransmitter signaling. Current Biology, 25(10), 1282–1295.

Majewska, A. and Yuste, R. (2001). Topology of gap junction networks in *C. elegans*. Journal of Theoretical Biology, 212, 155–167.

Morgan, J.L. and Lichtman, J.W. (2014). Why not connectomics? Nature Methods, 10(6), 494-500.

Portereiko, M.F. and Mango, S.E. (2001). Early Morphogenesis of the *Caenorhabditis elegans* Pharynx. Developmental Biology, 233, 482-494.

Reigl, M., Alon, U., and Chklovskii, D.B. (2004) Search for computational modules in the *C. elegans* brain. BMC Biology, 2, 25.

Seung, S. (2012). Connectome: How the Brain's Wiring Makes Us Who We Are. Houghton-Mifflin, New York.

Sohn, Y., Choi, M-K., Ahn, Y-Y., Lee, J., and Jeong, J. (2011). Topological Cluster Analysis Reveals the Systemic Organization of the *Caenorhabditis elegans* Connectome. PLoS Computational Biology, 7(5), e1001139.

Soto, M.C., Qadota, H., Kasuya, K., Inoue, M., Tsuboi, D., Mello, C.C., and Kaibuchi, K. (2002). The GEX-2 and GEX-3 proteins are required for tissue morphogenesis and cell migrations in *C. elegans*. Genes and Development, 16, 620-632.

Sulston, J.E., Schierenberg, E., White, J.G., and Thomson, J.N. (1983). The Embryonic Cell Lineage of the Nematode *Caenorhabditis elegans*. Developmental Biology, 100, 64-119.

Towlson, E.K., Vertes, P.E., Ahnert, S.E., Schafer, W.R., and Bullmore, E.T. (2013). The Rich Club of the *C. elegans* Neuronal Connectome. Journal of Neuroscience, 33(15), 6380-6387.

Varier, S. and Kaiser, M. (2011). Neural Development Features: Spatio-Temporal Development of the *Caenorhabditis elegans* Neuronal Network. PLoS Computational Biology, l7(1), e1001044. https://doi.org/10.1371/journal.pcbi.1001044.

Varshney, L.R., Chen, B.L., Paniagua, E., Hall, D.H., and Chklovskii, D.B. (2011). Structural Properties of the *Caenorhabditis elegans* Neuronal Network. PLoS Computational Biology, 7(2), e1001066.

White, J.G., Southgate, E., Thomson, J.N., and Brenner, S. (1986). The structure of the nervous system of the nematode *Caenorhabditis elegans*. Philosophical Transactions of the Royal Society of London B, 314, 1–340.